However, the rate constant for replacement of $PPh_3$ on $HFe_3(\mu\text{-}CNMe_2)(CO)_9(PPh_3)$ by CO (1 atm, $k_{obs}$ ca. $1 \times 10^{-4}$ $s^{-1}$ at 40 °C) is on the same order as that for CO dissociation from $HFe_3(\mu\text{-}CNMe_2)(CO)_{10}$. If the relative rates of ligand dissociation from the Fe center of $HFeRu_2(\mu\text{-}CNMe_2)(CO)_9L$ (L = CO, $PPh_3$) are similar to those from the $Fe_3$ analog, then this mechanism is ruled out because a significant quantity of the Fe-substituted isomer should be observed during the reaction if the rate constants for $PPh_3$ substitution on Fe and $PPh_3$ dissociation from Fe are comparable.

**Mechanism 2 (Figure 6, Path a).** Isomerization of the intermediate $HFeRu_2(\mu\text{-}CNMe_2)(CO)_9$ occurs to place Ru in the unique position. The $C_1$ and $Cs$ isomers of $HFeRu_2(\mu\text{-}CX)(CO)_{10}$ are in equilibrium, and it would not be surprising if isomerization of the intermediate is also rapid. Attack by $PPh_3$ on the Ru atom of the less stable $C_1$ isomer may be preferred on steric grounds.

**Mechanism 3 (Figure 6, Path b).** Attack by $PPh_3$ at the Fe atom generates $HFeRu_2(\mu\text{-}CNMe_2)(CO)_9(PPh_3)$ with substitution on Fe in the n-e site. Migration by $PPh_3$ to Ru and by CO from Ru to Fe would then generate the observed b-e product substituted on Ru. Precedent for phosphine migration has been recently provided by Puddephatt;[17] $PR_3$ ligands have been found to undergo rapid intramolecular migrations between the three Pt atoms of $[Pt_3(\mu_3\text{-}CO)(\mu\text{-}PPh_2CH_2PPh_2)_3(PR_3)]^+$. However, $PR_3$ intrametallic migration has not been observed in saturated cluster systems. Furthermore, the close similarity between the rate constants for n-e → b-e isomerizations of $HRu_3(\mu\text{-}CNMe_2)(CO)_9(ER_3)$ (E = P, As, Sb) suggests that $ER_3$/CO intramolecular, intermetallic exchange is not involved in the mechanism.[14]

**Mechanism 4 (Figure 6, Path c).** If the structure of the intermediate retains the $C_s$ symmetry of the $HM_3(\mu\text{-}CNMe_2)$ core, attack by $PPh_3$ might occur directly on one of the bridged Ru atoms, concomitant with hydride and methylidyne migration, to generate the n-e-substituted isomer, which could then rearrange to the preferred b-e isomer. Presumably, the same mechanism would then apply for substitution on $HRu_3(CNMe_2)(CO)_{10}$.

At this time we have no basis for distinction among mechanisms 2–4. All of these include intramolecular, intermetallic ligand migrations. Such migrations have also been proposed in a number of earlier studies of substitution on mixed-metal clusters. Atwood and Shojaie invoked CO migration to account for the ligand substitution behavior of $Ru_{3-n}Fe_n(CO)_{12}$.[3] Unsaturated intermediates containing bridging CO ligands, for example, $MnRe(CO)_9$,[18] $CpMoMn(CO)_7$,[19] and $Ru_3(CO)_{11}$,[20] have been identified by matrix isolation studies. It is becoming apparent that unsaturated metal cluster intermediates frequently contain bridging ligands or undergo facile rearrangements, making the reactive metal site difficult to identify. Studies of mixed-metal clusters are necessary to reveal these complicating mechanistic features.

**Acknowledgment.** This work was supported by Grant CHE8900921 from the National Science Foundation.

OM9202783

(17) Bradford, A. M.; Douglas, G.; Manojlovic-Muir, L.; Muir, K. W.; Puddephatt, R. J. *Organometallics* **1990**, *9*, 409.

(18) Firth, S.; Hodges, P. M.; Poliakoff, M.; Turner, J. J. *Inorg. Chem.* **1986**, *25*, 4608.

(19) Pope, K. R.; Wrighton, M. S. *Inorg. Chem.* **1987**, *26*, 2321.

(20) Bentsen, J. G.; Wrighton, M. S. *J. Am. Chem. Soc.* **1987**, *109*, 4530.

# Structure and Bonding in Bis(stannylene) Adducts of Zirconocene and 1,1′-Dimethylzirconocene

Warren E. Piers,*[1] Randy M. Whittal,[1] George Ferguson,[1] John F. Gallagher,[1] Robert D. J. Froese,[1] Henry J. Stronks,[2] and Peter H. Krygsman[2]

*Guelph-Waterloo Centre for Graduate Work in Chemistry, Guelph Campus, Department of Chemistry and Biochemistry, University of Guelph, Guelph, Ontario, Canada N1G 2W1, and Bruker Spectrospin (Canada) Ltd., 555 Steeles Avenue East, Milton, Ontario, Canada L9T 1Y6*

*Received July 28, 1992*

Decomposition of in situ generated $Cp'_2Zr(n\text{-}Bu)_2$ in the presence of 2 equiv of Lappert's stannylene $Sn[CH(SiMe_3)_2]_2$ yields the products $Cp'_2Zr\{Sn[CH(SiMe_3)_2]_2\}_2$ (Cp′ = $C_5H_5$ (**1a**, 42%), $C_5H_4CH_3$ (**1b**, 52%)). The $^{119}Sn$ NMR resonance for **1a** appears at +1677.6 ppm relative to $Me_4Sn$, with satellites arising from coupling to an adjacent $^{117}Sn$ nucleus ($^2J_{^{117}Sn}$ = 630 Hz). The compound **1b** was the subject of a single-crystal X-ray structure determination. It crystallizes in the space group $C2/c$ (No. 15) with $a$ = 25.455 (14) Å, $b$ = 11.563 (3) Å, $c$ = 19.471 (11) Å, $\beta$ = 93.46 (5)°, $V$ = 5721 (5) Å$^3$, and $Z$ = 4. Refinement of 231 variables on 3529 reflections observed ($I > 3.0\sigma(I)$) converged to $R$ = 0.048 and $R_w$ = 0.072. The molecule has pseudotetrahedral geometry at the zirconium atom with a 2-fold axis bisecting the Cp–Zr–Cp and Sn–Zr–Sn angles, two equivalent Zr–Sn bonds of 2.8715 (11) Å, and an Sn–Sn separation of 4.236 Å. Extended Hückel molecular orbital calculations show that there is significant $\pi$ bonding between zirconium and tin in these complexes.

## Introduction

Unearthing new examples of the periodicity inherent in the chemistry of the elements of the periodic table is a never-ending source of delight for chemists of all subdisciplines. Particularly striking are the parallels between the organometallic chemistry of the early transition metals and their corresponding groups in the p block of the periodic table. For example, a strong connection exists between organoscandium and organoaluminum chemistry;[3]

(1) Guelph-Waterloo Centre for Graduate Work in Chemistry, Guelph Campus.

(2) Bruker Spectrospin (Canada) Ltd.

(3) Piers, W. E.; Shapiro, P. J.; Bunel, E. E.; Bercaw, J. E. *Synlett.* **1990**, *1*, 74.

0276-7333/92/2311-4015$03.00/0 

also notable is the link between ylide derivatives of phosphorus, so-called Wittig reagents, and alkylidene complexes of tantalum.[4] While strong analogies in both the chemistry and structures exist between compounds of related groups, the presence of empty, low-lying d orbitals adds a dimension to the observed chemistry of the transition-metal compounds not present in their main-group cousins, such that often catalytic transformations are possible in addition to stoichiometric processes.

Clear examples of chemical analogies between group 4 organometallics and group 14 derivatives are rarer than the above-mentioned group 3/13 and 5/15 examples, possibly because of the unusually diverse nature of the chemistry associated with the group 14 elements. Nonetheless, conspicuous structural similarities exist between compounds of elements in the two groups. Spurred by the fascinating chemistry of heavy-element olefin analogs *within* group 14,[5] we became interested in stretching the analogy to include what might be thought of as a group 4/14 version of an olefin, namely "$R_2M{=}M'R'_2$", where M is a group 4 metal and M' a group 14 heavy element. Of the many conceivable routes to such a species, formation by the coupling of two carbene-like fragments appeared the most straightforward, since a variety of well-defined, monomeric germylenes and stannylenes are known[6] and a convenient method of generating a source of "$Cp_2Zr^{II}$" in situ was recently disclosed.[7] In fact, "$Cp_2Zr^{II}$" couples with 2 equiv of Lappert's bulky stannylene ligand $Sn[CH(SiMe_3)_2]_2$,[8] forming the title bis(stannylene) adducts of zirconocene.[9] Herein we report the full synthetic details for these adducts, their complete characterization, and an EHMO description of bonding within the molecules.

## Experimental Section

**General Considerations.** Details of our general procedures are reported elsewhere.[10] Zirconocene dichloride and $ClCH(SiMe_3)_2$ were purchased from Aldrich Chemicals and used without further purification, while 1,1'-dimethylzirconocene dichloride,[11] $Cp_2Zr(CH_3)_2$,[12] $BrCH(SiMe_3)_2$,[13] and $Sn\{CH(SiMe_3)_2\}_2$[14] were obtained according to published procedures.

$^1H$ and $^{13}C\{^1H\}$ NMR spectra were obtained on a Varian Gemini 200 or Unity 400. Proton spectra were collected with at least a 10-s relaxation delay to obtain accurate integrations of the cyclopentadienyl protons. Variable-temperature NMR experiments were performed on samples sealed in 5- or 10-mm NMR tubes under ~700 mm of purified argon. ESR measurements were taken using a Varian E-109 instrument. Microanalyses were performed by Onieda Research Services, Inc., One Halsey Rd., Whitesboro, NY 13492.

**Syntheses of $Cp'_2Zr[Sn\{CH(SiMe_3)_2\}_2]_2$ (Cp = $C_5H_5$ (1a), $CH_3C_5H_4$ (1b)).** To a solution of $Cp_2ZrCl_2$ (1.0 g, 3.4 mmol) in THF (30 mL) was added 4.4 mL of a 1.6 M solution of *n*-BuLi (Aldrich, 7.0 mmol) at −78 °C. To the resulting yellow solution of $Cp_2Zr(n\text{-}Bu)_2$ was added via syringe a solution of $Sn[CH(SiMe_3)_2]_2$ (3.06 g, 7.0 mmol, keep in the dark until addition) in THF (20 mL). This reaction mixture was warmed slowly to 0 °C, at which temperature it was stirred for 1 h. A gradual darkening of the reaction mixture was observed during this period. The THF was then removed in vacuo and the residue extracted twice with hexanes (30 mL), yielding an intensely blue filtrate. The hexane was pumped off, leaving a free-flowing blue powder of crude **1a** (2.7 g, 71%, >90% pure). Samples that were 95% pure could be obtained by recrystallization from hexanes at −78 °C (1.6 g, 42%). An identical procedure using $(C_5H_4Me)_2ZrCl_2$ yielded **1b** (crude yield, 72%; pure compound, 52%). $^1H$ NMR ($C_6D_6$, ppm; **1a**): $C_5H_5$, 5.36 (s, 10 H); $CH(SiMe_3)_2$, broad, unobserved at room temperature; $CH(SiMe_3)_2$, 0.37 (s, 72 H). $^{13}C\{^1H\}$ NMR ($C_6D_6$, ppm; **1a**): $C_5H_5$, 94.32; $CH(SiMe_3)_2$, 5.62; $CH(SiMe_3)_2$, 3.76. $^1H$ NMR ($C_6D_6$, ppm; **1b**): $C_5H_4Me$, 5.71; 5.34 (br t, 8 H); $C_5H_4Me$, 1.59 (s, 6 H); $CH(SiMe_3)_2$, broad, unobserved at room temperature; $CH(SiMe_3)_2$, 0.38 (s, 72 H). $^{13}C\{^1H\}$ NMR ($C_6D_6$, ppm; **1b**): $C_5H_4Me$, 112.65, 98.92, 90.79; $C_5H_4Me$, 14.40; $CH(SiMe_3)_2$, 5.81; $CH(SiMe_3)_2$, 3.83. Note: analytically pure samples within the normally accepted range were not obtainable owing to the presence of small amounts of unremovable impurities and incomplete combustion. Anal. Calcd for $C_{38}H_{86}Si_8Sn_2Zr$ (**1a**): C, 41.62; H, 7.90. Found: C, 39.59; H, 6.88. Calcd for $C_{40}H_{90}Si_8Sn_2Zr$ (**1b**): C, 42.72; H, 8.07. Found: C, 41.87; H, 7.65.

**Reaction of $Cp_2Zr(CH_3)_2$ with $Sn\{CH(SiMe_3)_2\}_2$.** A sealable 5-mm NMR tube was loaded with $Cp_2Zr(CH_3)_2$ (6.9 mg, 0.027 mmol) and $Sn\{CH(SiMe_3)_2\}_2$ (12.0 mg, 0.027 mmol) and attached via a 180° needle valve to a vacuum line. The tube was evacuated, and ~0.6 mL of dry benzene-$d_6$ was vacuum transferred onto the two solids. The tube was flame-sealed and warmed to room temperature; an orange solution of a 1:1 adduct between the starting materials resulted. $^1H$ NMR ($C_6D_6$, ppm): $C_5H_5$, 5.94 (s, 10 H); $Zr{-}CH_3$ (exo), 0.54 (s, 3 H); $CH(SiMe_3)_2$ (exo or endo), 0.33 (s, 18 H); $CH(SiMe_3)_2$ (exo or endo), 0.25 (s, 18 H); $Zr{-}CH_3$ (endo), −0.24 (s, 3 H, $^3J_{Sn}$ = 5.3 Hz); $CH(SiMe_3)_2$, broad, unobserved at room temperature.

**Tin Nuclear Magnetic Resonance Experiments.** $^{119}Sn$ and $^{117}Sn$ NMR spectra were obtained on a Bruker AC-F 200 instrument equipped with a 10-mm broad-band probe head at 74.545 and 71.251 MHz, respectively, using $Sn(CH_3)_4$ at 0.0 ppm as an external standard. Spectra were recorded with a spectrum width of 29 412 Hz and spectrum digital resolution of 1.8 Hz per point. A 90° pulse width and a relaxation delay of 1 s were used for a total of 20 000 transients collected. $T_1$ measurements were performed at 273 K via the inversion recovery pulse sequence, revealing a very short $T_1$ of 12 ms for **1a**. Since inverse-gated $^1H$ decoupling caused no change in the appearance of the Sn resonance, indicating that any $^1H{-}Sn$ coupling is well within the observed Sn line widths, spectra were recorded with no decoupling. The FID was processed with an exponential multiplication of 20 Hz, except when accurate line widths at half-height were measured.

**X-ray Analysis of $Cp'_2Zr[Sn\{CH(SiMe_3)_2\}_2]_2$.** A dark red crystal of **1b** (grown from toluene solution at 0 °C in a sealed tube) was mounted in a glass capillary under an atmosphere of argon. Accurate unit cell parameters were determined on a CAD4 diffractometer from a least-squares refinement of 25 independent reflections in the range $16 < \theta < 30°$. A total of 4608 reflections were measured ($h$, −29 to +28; $k$, 0–13; $l$ 0–22), in the range $2 < 2\theta < 48°$ ($\omega$–$2\theta$ scans, $\omega$-scan width (0.7 + 0.35 tan $\theta$)°, graphite-monochromated Mo K$\alpha$ radiation. The data were corrected for Lorentz, polarization, and absorption effects (minimum and maximum transmission factors of 0.68 and 0.83). Three intensity control reflections measured at 1-h intervals decayed by 5% during data collection, and this was allowed for using the five-point smoothing function of the NRCVAX data reduction program. The structure was solved by the heavy-atom method. All non-hydrogen atoms were located from an *E*-map and refined anisotropically. All hydrogen atoms were positioned at calculated geometries and included in the structure factor calculations as riding atoms on the relevant carbon atoms (C–H = 0.95 Å). A total of 4608 reflections were measured, 4467 of which were unique and 3529 with $I > 3\sigma(I)$ labeled observed and used in structure solution and refinement. The space group $C2/c$ was confirmed from systematic absenses ($h0l$, $l = 2n + 1$; $0k0$, $k = 2n + 1$) and

(4) Schrock, R. R. *J. Organomet. Chem.* **1986**, *300*, 249.
(5) (a) West, R. *Angew. Chem., Int. Ed. Engl.* **1987**, *26*, 1201. (b) Barrau, J.; Escudie, J.; Satgé, J. *Chem. Rev.* **1990**, *90*, 283.
(6) Lappert, M. F. *Silicon, Germanium, Tin Lead Cmpd.* **1986**, *9*, 129.
(7) Negishi, E.; Holmes, S. J.; Tour, J. M.; Miller, J. A.; Cederbaum, R. E.; Swanson, D. R.; Takahashi, T. *J. Am. Chem. Soc.* **1989**, *111*, 3336.
(8) Davidson, P. J.; Harris, D. H.; Lappert, M. F. *J. Chem. Soc., Dalton Trans.* **1976**, 2268.
(9) Whittal, R.; Gallagher, J. F.; Ferguson, G.; Piers, W. E. *J. Am. Chem. Soc.* **1991**, *113*, 9867.
(10) Piers, W. E.; Koch, L.; Ridge, D. S.; MacGillivray, L. R.; Zaworotko, M. *Organometallics* **1992**, *11*, 3148.
(11) Jordan, R. F.; LaPointe, R. E.; Bradley, P. K.; Baenziger, N. *Organometallics* **1989**, *8*, 2892.
(12) Samuel, E.; Rausch, M. D. *J. Am. Chem. Soc.* **1973**, *95*, 6263.
(13) Wiberz, N.; Wagner, G. *Chem. Ber.* **1986**, *119*, 1462.
(14) Davidson, P. J.; Harris, D. H.; Lappert, M. F. *J. Chem. Soc., Dalton Trans.* **1976**, 2268.

**Table I. Summary of Data Collection, Structure Solution, and Refinement Details for 1b**

| | |
|---|---|
| formula | $C_{40}H_{90}Si_8ZrSn_2$ |
| fw | 1124.4 |
| color, habit | dark red, block, in sealed capillary under Ar |
| cryst size, mm | 0.25 × 0.55 × 0.55 |
| cryst syst | monoclinic |
| *a*, Å | 25.455 (14) |
| *b*, Å | 11.563 (3) |
| *c*, Å | 19.471 (11) |
| *β*, deg | 93.46 (5) |
| *V*, Å$^3$ | 5721 (5) |
| space group | *C*2/*c* |
| *Z* | 4 |
| *F*(000) | 2328 |
| $d_{calc}$, g cm$^{-3}$ | 1.31 |
| $\mu$, cm$^{-1}$ | 12.3 |
| min, max abs cor | 0.68, 0.83 |
| diffractometer | Enraf-Nonius, CAD4 |
| radiation | Mo K$\alpha$ ($\lambda$ = 0.7093 Å) |
| monochromator | graphite |
| 2$\theta$ range, deg | 4 - 48 |
| temp, °C | 293 |
| *hkl* range of rflns | −29 to +28, 0–13, 0–22 |
| no. of reflns measd | 4608 |
| no. of unique rflns | 4467 |
| $R_{int}$ | 0.02 |
| no. of reflns with $I > 3\ \sigma(I)$ | 3529 |
| no. of variables in LS | 231 |
| $k$ in $w = 1/(\sigma^2F_o + kF_o^2)$ | 0.0025 |
| $R$, $R_w$, GOF | 0.048, 0.072, 1.24 |
| density range in final Δ map, e Å$^{-3}$ | −1.23/+0.73 |
| final shift/error ratio | 0.001 |

**Table II. Positional and Thermal Parameters and Their Esd's for 1b**

| atom | *x* | *y* | *z* | *B*(iso),[a] Å$^2$ |
|---|---|---|---|---|
| Sn | 0.08147 (1) | 0.09990 (4) | 0.23338 (2) | 2.80 (2) |
| Zr | 0.00000 (0) | −0.06778 (7) | 0.00000 (0) | 3.05 (4) |
| Si(1) | 0.09271 (9) | 0.28281 (21) | 0.08654 (12) | 5.13 (10) |
| Si(2) | 0.15754 (8) | 0.05270 (21) | 0.09710 (10) | 4.32 (9) |
| Si(3) | 0.12244 (7) | 0.31673 (17) | 0.34696 (12) | 4.37 (9) |
| Si(4) | 0.20156 (7) | 0.10759 (17) | 0.33625 (10) | 3.72 (8) |
| C(1) | −0.0490 (3) | −0.2125 (6) | 0.1728 (5) | 5.2 (4) |
| C(2) | 0.0033 (4) | −0.2291 (10) | 0.1652 (6) | 7.6 (5) |
| C(3) | 0.0242 (3) | −0.1326 (13) | 0.1351 (5) | 7.9 (6) |
| C(4) | −0.0181 (4) | −0.0516 (8) | 0.1248 (4) | 5.8 (4) |
| C(5) | −0.0617 (3) | −0.1032 (6) | 0.1472 (4) | 4.0 (3) |
| C(6) | −0.0906 (5) | −0.2973 (9) | 0.1990 (6) | 9.4 (7) |
| C(7) | 0.1241 (3) | 0.1715 (6) | 0.1444 (4) | 3.7 (3) |
| C(8) | 0.1315 (2) | 0.1615 (6) | 0.3242 (3) | 3.2 (3) |
| C(11) | 0.0856 (4) | 0.4239 (8) | 0.1322 (6) | 6.6 (5) |
| C(12) | 0.1339 (5) | 0.3181 (11) | 0.0126 (6) | 9.8 (7) |
| C(13) | 0.0276 (4) | 0.2372 (9) | 0.0470 (5) | 7.0 (5) |
| C(21) | 0.2226 (3) | 0.1019 (9) | 0.0695 (5) | 6.4 (5) |
| C(22) | 0.1159 (3) | 0.0020 (9) | 0.0186 (4) | 6.2 (4) |
| C(23) | 0.1719 (3) | −0.0789 (7) | 0.1501 (4) | 4.9 (4) |
| C(31) | 0.1711 (3) | 0.4124 (7) | 0.3090 (7) | 7.5 (6) |
| C(32) | 0.0554 (3) | 0.3691 (7) | 0.3177 (5) | 5.5 (4) |
| C(33) | 0.1278 (4) | 0.3380 (10) | 0.4417 (6) | 8.1 (6) |
| C(41) | 0.2441 (3) | 0.1549 (7) | 0.2666 (4) | 4.8 (4) |
| C(42) | 0.2051 (3) | −0.0530 (7) | 0.3432 (4) | 4.5 (3) |
| C(43) | 0.2351 (3) | 0.1590 (8) | 0.4184 (4) | 5.3 (4) |

[a] *B*(iso) is the mean of the principal axes of the thermal ellipsoid.

subsequent successful refinement. The final refinement cycle included 231 variable parameters: $R = 0.048$, $R_w = 0.072$, goodness of fit 1.24, $w = 1/[\sigma^2(F_o) + 0.0025(F_o)^2]$. The maximum shift/esd is <0.001, and the maximum density in the final difference map is 0.73 e Å$^{-3}$. Scattering factors and anomalous dispersion corrections are from ref 15. All calculations were performed on a Silicon Graphics 4D-380 mainframe computer using the NRCVAX suite of programs.[16] Crystal data are given in Table I, and atomic coordinates and selected bond lengths and angles are given in Tables II and III, respectively. Figure 2 is a view of the molecule prepared using Chem 3D Plus.[17]

**Molecular Orbital Calculations.** Extended Hückel calculations were performed using the CACAO program package.[18] Orbital parameters for zirconium[19] and tin[20] were obtained from literature sources. The geometry of $Cp_2Zr(SnMe_2)_2$ was idealized at $C_{2v}$, with geometrical distances and angles obtained from the X-ray crystallographic data for **1b**.

## Results and Discussion

**Synthesis.** A THF solution at −78 °C of $Cp'_2Zr(n\text{-}C_4H_9)_2$ (Cp′ = $C_5H_5$ (**a**), $CH_3C_5H_4$ (**b**)) was generated in the usual manner[21] from the corresponding dichlorides and $n$-$C_4H_9Li$. A separately prepared solution containing 2 molar equiv of the monomeric stannylene $Sn[CH(SiMe_3)_2]_2$ was then added dropwise via syringe to the cold dibutylzirconocene solution (eq 1). During the first half of this

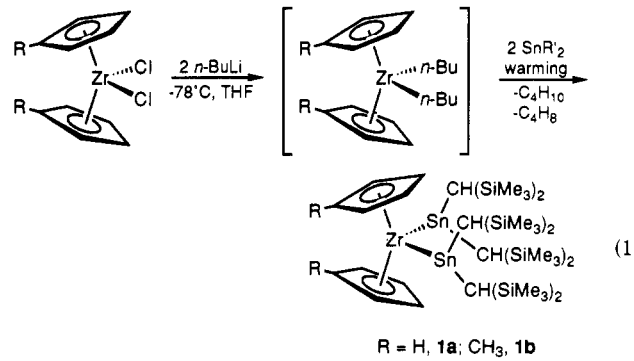


(1)

R = H, **1a**; $CH_3$, **1b**

addition, the intense red color of the stannylene was observed to dissipate rapidly, forming a light orange solution. The second equivalent of stannylene produced a more deeply colored reaction mixture, presumably owing to the presence of free stannylene in the reaction medium. The admixture was then warmed gradually to 0 °C and stirred for 2 h; during this warming phase, the reaction mixture slowly darkened until it appeared black. Removal of the THF followed by extraction with hexanes yielded a deep blue filtrate from which red-purple microcrystals of the bis(stannylene) adducts **1a** and **1b** could be isolated in moderate yields. Both of these compounds exhibit high solubility in hydrocarbon solvents, as well as donor solvents such as THF and $Et_2O$, and slowly react with methylene chloride to form colorless Zr(IV) and Sn(IV) products. Hexane solutions of **1a** and **1b** ($\sim 10^{-2}$ M) decolorize slowly over the course of a few minutes when exposed to the atmosphere. While complexes of alkyl- and aminostannylene ligands with the later transition metals are well established,[22] compounds **1a** and **1b** represent the first examples of a group 4 complex with these ligands; indeed, a stannylene adduct of $Cp_2ScCH_3$ is the only other reported early-transition-metal stannylene compound.[23]

In order to obtain optimum yields of pure product in the sequence described above, care must be taken to ensure

(15) *International Tables for X-ray Crystallography*; Kynoch Press: Birmingham, England, 1974; Vol. IV.

(16) Gabe, E. L.; Le Page, Y.; Charland, J.-P.; Lee, F. L.; White, P. S. *J. Appl. Crystallogr.* **1989**, *22*, 384.
(17) Chem 3D Plus, Version 3.0; Cambridge Scientific Computing: 875 Massachussetts Ave., Suite 61, Cambridge, MA 02139.
(18) Mealli, C.; Prosperpio, D. M. *J. Chem. Educ.* **1990**, *67*, 3399.
(19) Tatsumi, K.; Nakamura, A.; Hofmann, P.; Stauffert, P.; Hoffmann, R. *J. Am. Chem. Soc.* **1985**, *107*, 4445.
(20) Hinze, J.; Jaffe, H. H. *J. Phys. Chem.* **1963**, *67*, 1501.
(21) Negishi, E.; Cederbaum, F. E.; Takahashi, T. *Tetrahedron Lett.* **1986**, *27*, 2829.
(22) Lappert, M. F.; Rowe, R. S. *Coord. Chem. Rev.* **1990**, *100*, 267.
(23) Lappert, M. F.; Power, P. P. *J. Chem. Soc., Dalton Trans.* **1985**, 51.

**Table III. Selected Bond Lengths and Angles for 1b[a]**

| | | | | | |
|---|---|---|---|---|---|
| | | Bond Lengths (Å) | | | |
| Sn–Zr | 2.8715 (11) | Sn–C(7) | 2.256 (7) | Sn–C(8) | 2.233 (6) |
| Zr–Cp | 2.196 (8) | C(1)–C(2) | 1.362 (14) | C(1)–C(5) | 1.390 (10) |
| C(1)–C(6) | 1.552 (15) | C(2)–C(3) | 1.381 (20) | C(3)–C(4) | 1.432 (17) |
| C(4)–C(5) | 1.356 (11) | Si(1)–C(7) | 1.858 (7) | Si(2)–C(7) | 1.886 (7) |
| Si(3)–C(8) | 1.866 (7) | Si(4)–C(8) | 1.892 (6) | Sn–Sn′ | 4.2364 |
| | | Bond Angles (deg) | | | |
| Zr–Sn–C(7) | 135.9 (2) | Zr–Sn–C(8) | 120.5 (2) | C(7)–Sn–C(8) | 102.4 (2) |
| Sn–Zr–Sn′ | 95.06 (4) | Sn–Zr–Cp | 108.0 (2) | | |
| Sn–Zr–Cp′ | 104.2 (2) | Cp–Zr–Cp′ | 131.5 (3) | | |
| Sn–C(7)–Si(1) | 120.8 (3) | Sn–C(7)–Si(2) | 111.1 (3) | Si(1)–C(7)–Si(2) | 113.5 (4) |
| Sn–C(8)–Si(3) | 115.0 (3) | Sn–C(8)–Si(4) | 118.7 (3) | Si(3)–C(8)–Si(4) | 114.6 (3) |
| C(2)–C(1)–C(5) | 107.3 (9) | C(2)–C(1)–C(6) | 129.6 (9) | C(5)–C(1)–C(6) | 122.9 (8) |
| C(1)–C(2)–C(3) | 109.7 (9) | C(2)–C(3)–C(4) | 106.4 (8) | C(3)–C(4)–C(5) | 106.9 (9) |
| C(1)–C(5)–C(4) | 109.7 (7) | | | | |

[a] Cp is the centroid of the cyclopentadienyl ring: C(1) through C(5). The prime refers to the following equivalent position: $-x, y, 0.5 - z$.

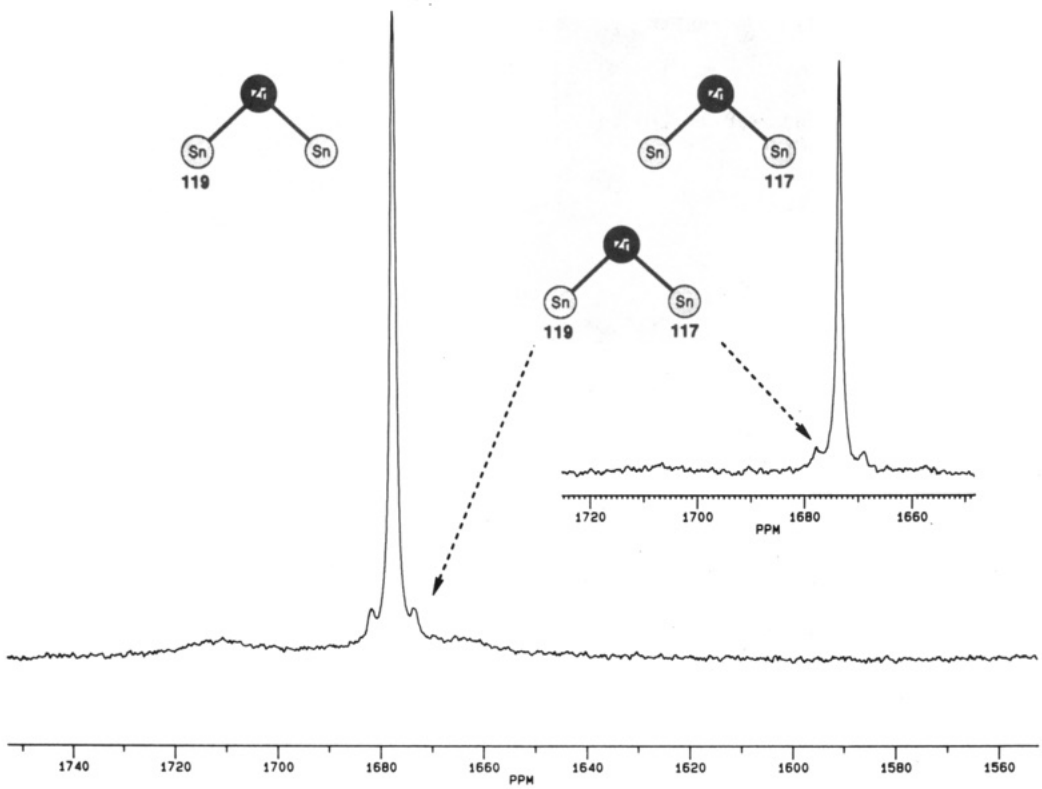


**Figure 1.** $^{119}Sn$ (74.545 MHz, bottom trace) and $^{117}Sn$ (71.251 MHz, inset) NMR spectra of $Cp_2Zr[Sn[CH(SiMe_3)_2]_2]_2$ (**1a**), recorded at −18 °C.

the integrity of the stannylene reagent. This seems an obvious point but is nontrivial due to the ready decomposition of $SnR_2$ upon irradiation with visible light (eq 2).[24]

$$2\ :Sn\{CH(SiMe_3)_2\}_2 \xrightarrow{h\upsilon} \cdot Sn\{CH(SiMe_3)_2\}_3 + 1/n\ [Sn\{CH(SiMe_3)\}]_n \quad (2)$$

Chemically significant amounts of the stable trialkylstannyl radical $\cdot SnR_3$ (identified by ESR spectroscopy)[25] are produced if the synthesis and handling of $SnR_2$ is performed without precautionary exclusion of visible light. It is therefore important to keep solutions of this ligand in the dark at all times prior to use in the syntheses of **1a,b**.

Mechanistic studies on the decomposition of $Cp_2Zr(n\text{-}Bu)_2$ by Negishi[26] and Waymouth[27] suggest that a non-dissociative β-hydrogen abstraction is the main pathway by which it decays. Loss of 1 equiv of butane leaves a "$Cp_2Zr$" synthon stabilized by an $\eta^2$-coordinated butene ligand; when generated in the presence of a suitable substrate, this reagent moderates an impressive array of transformations, including reductive coupling of organic functionalities[7] and hydrosilation of olefins.[27] Alternatively, it may be trapped with a phosphine donor to form stable phosphine/butene mixed adducts of zirconocene.[28] These studies suggest that the zirconocene olefin adduct is intercepted by $PR_3$ *after* the β-hydrogen-abstraction step. In contrast, our evidence points to stannylene coordination to dibutylzirconocene *before* β-hydrogen re-

(24) Hudson, A.; Lappert, M. F.; Lednor, P. W. *J. Chem. Soc., Dalton Trans.* **1976**, 2369.
(25) Davidson, P. J.; Hudson, A.; Lappert, M. F.; Lednor, P. W. *J. Chem. Soc., Chem. Commun.* **1973**, 829.
(26) Negishi, E.; Swanson, D. R.; Takahashi, T. *J. Chem. Soc., Chem. Commun.* **1990**, 1254.
(27) Kesti, M. R.; Waymouth, R. M. *Organometallics* **1992**, *11*, 1095.
(28) (a) Binger, P.; Müller, P.; Benn, R.; Rufinska, A.; Gabor, B.; Krüger, C.; Betz, P. *Chem. Ber.* **1989**, *122*, 1035. (b) Takahashi, T.; Murakami, M.; Kunishige, M.; Saburi, M.; Uchida, Y.; Kozawa, K.; Uchida, T.; Swanson, D. R.; Negishi, E. *Chem. Lett.* **1989**, 761.

moval takes place. The rapid dissipation of the stannylene solution's distinctive red color upon addition of the first equivalent to solutions of dibutylzirconocene led us to speculate on the possibility of adduct formation between the stannylene and the dialkylzirconocene. Although we have not directly observed this particular adduct, we have observed (by $^1$H NMR) facile complex formation in solution between $Sn\{CH(SiMe_3)_2\}_2$ and $Cp_2Zr(CH_3)_2$ when the two are mixed together in benzene at room temperature (eq 3). The presence of two peaks for the trimethylsilyl

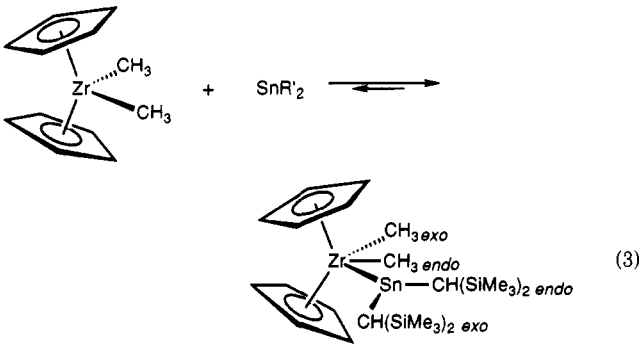


(3)

protons (endo and exo) and resonances for endo (−0.24 ppm, $^3J_{Sn}$ = 5.3 Hz) and *exo* (0.54 ppm) Zr–$CH_3$ groups in the proton NMR spectrum, along with complete loss of signals due to starting materials, indicate that complex formation is complete under these conditions. Interestingly, solutions of this dimethylzirconocene–stannylene adduct decompose over a period of days to the bis(stannylene)–zirconocene adduct **1a**, $Cp_2Zr(CH_3)_2$, and presumably ethane, although this was not detected.[29] On the basis of these observations we suspect that an adduct forms between the first equivalent of stannylene and dibutylzirconocene prior to β-hydrogen abstraction and that the second equivalent of ligand displaces coordinated butene.[30]

**Solution Characterization.** It was anticipated that the steric properties of the stannylene donor would preclude formation of a bis(ligand) complex; nevertheless, $^1$H and $^{13}C\{^1H\}$ NMR data were consistent with the incorporation of 2 equiv of the stannylene ligand into zirconium's coordination environment from the relative integrals of the Cp vs the trimethylsilyl peaks. A significant question left unanswered by the $^1$H and $^{13}C\{^1H\}$ NMR data was whether or not the stannylenes had been reductively coupled by zirconium(II), generating a tin–tin bond. While the color of the complexes ($\lambda_{max}$ for **1a** 610 nm; $\epsilon \approx 1.3 \times 10^3$) is indicative of a formally zirconium(II) center in both **1a** and **1b**, simple molecular orbital considerations (vide infra) suggest that a σ interaction between the two tin atoms would be possible upon reduction of the stannylene ligands by Zr(II). To answer this question, $^{119}$Sn NMR measurements on **1a** were performed.

Direct detection of the $^{119}$Sn resonance for **1a** was accomplished on a saturated (ca. 0.1 M) toluene solution of **1a** at 74.631 MHz and 0 °C (Figure 1). The signal appears at +1677.6 ppm relative to $Me_4Sn$ and, consistent with the presence of two stannylene ligands, exhibits satellites due to coupling to an adjacent $^{117}$Sn nucleus ($^2J_{^{119}Sn-^{117}Sn}$ = 630 Hz). The presence of $^{119}$Sn satellites in the $^{117}Sn\{^1H\}$ NMR spectrum of **1a** (inset, Figure 1) with an identical coupling constant confirmed this assignment. The magnitude of this coupling constant verifies the intuitive judgment against any direct Sn–Sn interaction based on the compound's color, since it falls well outside the normal range of ~2500–4500 Hz observed for $^1J_{^{119}Sn-^{117}Sn}$ couplings.[31] The value observed is compatible with a cisoid Sn–M–Sn functionality.[31,32]

Several other interesting features of these spectra deserve comment. The low-field chemical shift for the tin atoms in this molecule indicates that they are among the most deshielded tin nuclei discovered to date. The free, *monomeric* stannylene $Sn\{CH(SiMe_3)_2\}_2$ itself resonates at +2328 ppm.[33] The related monomeric stannylenes Sn(2,4,6-*i*-$Pr_3C_6H_2)_2$ and $Sn\{N(SiMe_3)_2\}_2$ exhibit tin chemical shifts of +1420[34] and +776ppm[35] respectively, relative to $Me_4Sn$. These, and other,[36] high-frequency shifts for stannylenes have been rationalized as deshielding by a circulation of charge from the molecular trigonal plane into the empty, unhybridized p orbital on tin.[35] Clearly, coordination of the dialkylstannylene to the zirconium center in "$Cp_2Zr$" shields the tin atoms relative to the free monomer; coordination of $Sn\{CH(SiMe_3)_2\}_2$ to a more electron-rich Rh(I) center in *cis*-$[RhCl(PPh_3)_2(SnR_2)]$ results in a similar, more pronounced upfield shift to +434 ppm.[22] A possible contributing factor to these upfield chemical shift changes upon stannylene coordination could be π-bonding between the transition metal and tin (vide infra).

The spectra shown in Figure 1 were recorded under optimized conditions (see Experimental Section). It was found that as the temperature of the sample was varied, the line width at half-height changed from 230 Hz at 27 °C to a minimum of 82 Hz at −18 °C. Further lowering of the temperature led to slight broadening due to viscosity effects. No coalescence of the signal was observed upon raising the temperature. In addition, a small effect (~+4 ppm) on the chemical shift was observed upon lowering the temperature. In our original report,[9] we disclosed the observed temperature dependence of the $^1$H NMR spectrum for **1a**. Cooling a sample of **1a** resulted in a coalescence of the singlet due to the trimethylsilyl protons on the stannylene ligand until, at −50 °C, four separate singlets were resolved (0.29, 0.31, 0.37, and 0.44 ppm). Initially, the signals at 0.29 and 0.31 ppm were not resolved, leading us to speculate on a fluxional process which involved rotation of one of the stannylene ligands into the plane defined by the zirconium and two tin atoms. In light of the variable-temperature $^{119}$Sn NMR experiment's failure to conclusively demonstrate an exchange process involving two chemically inequivalent tin environments, we now interpret the variable-temperature proton NMR results in terms of restricted rotation about the Sn–C bonds of the stannylene ligand. This phenomenon is common in organometallic compounds containing the very bulky bis(trimethylsilyl)methyl ligand.[37] A low-energy static solution structure similar to that observed in the solid state (vide infra) would produce the four separate

(29) (a) Lewis-base-induced reductive elimination has been employed to prepare bis(phosphine) adducts of zirconocene.[29b] Not surprisingly, the kinetically more favored elimination of methane from $Cp_2Zr(CH_3)H$[29c] when treated with $Sn\{CH(SiMe_3)_2\}_2$ is much more facile. Indeed, this route represents a viable alternative synthesis of the title compounds. (b) Gell, K. I.; Schwartz, J. *J. Am. Chem. Soc.* **1981**, *103*, 2687. (c) Jordan, R. F.; Bajgur, C. S.; Dasher, W. E.; Rheingold, A. L. *Organometallics* **1987**, *6*, 1041.

(30) No *n*-octane was detected indicating that reductive elimination of *n*-octane is not a competing pathway for the production of "$Cp_2Zr[Sn\{CH(SiMe_3)_2\}_2]$".

(31) Wrackmeyer, B. *Annu. Rep. NMR Spectrosc.* **1985**, *16*, 73.

(32) Holt, M. S.; Wilson, W. L.; Nelson, J. H. *Chem. Rev.* **1989**, *89*, 11.

(33) Zilm, K. W.; Lawless, G. A.; Merrill, R. M.; Millar, J. M.; Webb, G. G. *J. Am. Chem. Soc.* **1987**, *109*, 7236.

(34) Weidenbrüch, M.; Schäfer, A.; Kilian, H.; Pohl, S.; Saak, W.; Marsmann, H. *Chem. Ber.* **1992**, *125*, 563.

(35) Wrackmeyer, B. *J. Magn. Reson.* **1985**, *61*, 536.

(36) $Sn[Fe(CO)_2Cp]_2$, 892.1 ppm: Duan, Z.; Lei, D.; Hampden-Smith, M. J. *Polyhedron* **1991**, *10*, 2105.

(37) Schaverien, C. J.; Nesbitt, G. J. *J. Chem. Soc., Dalton Trans.* **1992**, 157.

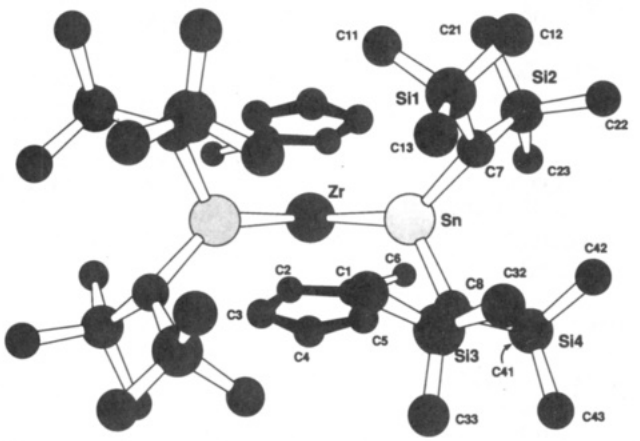


**Figure 2.** Chem 3D diagram and atom-numbering scheme for $Cp'_2Zr[Sn[CH(SiMe_3)_2]_2]_2$ (**1b**).

$SiMe_3$ environments observed in the low-temperature $^1H$ NMR spectrum.[38]

Finally, in both spectra shown in Figure 1, a broad, unsymmetrical pattern is evident in the base line around the main tin resonance. The presence of this feature in both spectra leads us to speculate that it arises from coupling of the tin nuclei with the quadrupolar $^{91}Zr$ nucleus (11.23% abundance; $I = {}^5/_2$).[39] Attempts were made to record the $^{91}Zr$ resonance for **1a**, but the signal is so broad that detection in solution was difficult and in any event provided little information regarding possible Zr–Sn coupling.[40]

**Solid-State Structure of 1b.** Although solution methods conclusively demonstrated the absence of a tin–tin interaction, we were interested in establishing the structural parameters associated with the zirconium–tin bond. The molecular structure of the 1,1′-dimethylzirconocene derivative **1b** is presented in Figure 2; selected bond distance and bond angle data are given in Table III, while crystal data and positional and isotropic thermal parameters are given in Tables I and II, respectively. The view of the molecule shown sights along a crystallographic 2-fold axis which bisects the Cp–Zr–Cp and Sn–Zr–Sn′ angles.

Most of the structural attributes of this complex arise from the considerable steric tension within the molecule as imposed by the large stannylene donors. For example, the Sn–Zr–Sn′ bond angle of 95.06 (4)° is significantly larger than the L–M–L range of 76–82° predicted[41] and found[42] in other $d^2$ $Cp_2ML_2$ complexes. The geometry about tin in the stannylene ligands is somewhat distorted from an ideal trigonal plane; the Zr–Sn–C(7) and C(7)–Sn–C(8) bond angles deviate significantly from 120° at 135.9 (2)° and 102.4 (2)°, respectively. These distortions shift the stannylene ligands in opposite directions with respect to the Sn–Zr–Sn′ plane, minimizing intramolecular nonbonded contacts. In addition, the alkyl groups are bent back slightly (9.67°) from the Zr–Sn vector; i.e., the Zr, Sn, C(7), and C(8) atoms are not coplanar. The Sn atom sits 0.155 Å above the plane defined by Zr, C(7), and C(8). It thus appears that, although orbitally and electronically feasible (vide infra), tin–tin bond formation in this complex has been arrested by the steric barrier associated with bringing the two tin centers to within reasonable bonding distance; in agreement with the $^{119}Sn$ NMR results, the substantive Sn–Sn separation of 4.236 Å precludes any direct tin–tin contact.

The most interesting piece of information is the Zr–Sn distance of 2.872 Å, a length which we believe may be considered "short" for a Zr–Sn bond. The orientation of the stannylene ligands, with $CH(SiMe_3)_2$ groups above and below the Sn–Zr–Sn′ plane, should allow for maximum $\pi$ overlap between the empty p orbitals on the two tin atoms and the filled $1a_1$ orbital of the $Cp_2Zr^{II}$ fragment (I). Since

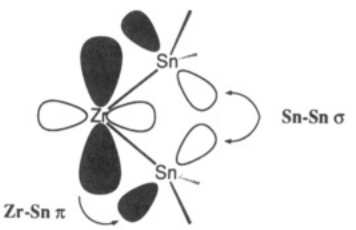


I

this orientation is also likely to be the most favorable from a steric point of view, the question of what role $\pi$ bonding plays in the Zr–Sn linkage is a significant one. In other transition-metal complexes containing the $Sn[CH(SiMe_3)_2]_2$ ligand, M–Sn multiple bonding has been invoked on the basis of a "short" M–Sn bond.[43,44] A paucity of data for Zr–Sn bond distances makes it difficult to judge whether a bond length of 2.872 Å may be considered as being shorter than a "standard" Zr–Sn single bond, but we offer the following observations. First, the only other known crystallographically characterized zirconium–tin complex is the Zr(II) complex $[(Ph_3Sn)_4Zr(CO)_4]^{2-}$, in which a considerably longer Zr–Sn distance of 3.086 Å was observed.[45] Second, a reasonable Zr(II)–Sn(IV) distance may be calculated at ~3.0 Å using a value of 1.6 Å[46] for a Zr(II) radius and 1.4 Å[47] for Sn(IV). Finally, the size requirements of Sn(II) are known to be greater than those of Sn(IV) by as much as 0.2 Å.[48] Thus, the available data do suggest that the Zr–Sn bonds in **1b** are shorter than expected for a normal Zr(II)–Sn(II) single bond, arguing for a significant $\pi$ component to the bonds in question. Admittedly, these arguments are qualitative at best; more

(38) It is not clear what causes the observed temperature dependence of the $^{119}Sn$ signal. We do note, however, that small amounts of unidentified paramagnetic impurities (~$10^{-7}$–$10^{-8}$ M) were detected (by ESR spectroscopy) in the sample on which the $^{119}Sn$ NMR measurements were made. These species appear to be Zr(III) compounds; no $^{\bullet}SnR_3$[25] was detected in the sample. While these impurities may be present in large enough amounts to affect the line width and the relaxation time (0.012 for **1a**, see Experimental Section), they do not provide an explanation for the large downfield chemical shift observed for **1a**.

(39) Brevard, C.; Granger, P. *Handbook of High Resolution Multinuclear NMR*; Wiley: New York, 1981; p 148.

(40) $^{91}Zr$ signals with acceptable line widths usually require a highly symmetric environment about the zirconium center: Sayer, B. G.; Hao, N.; Denes, G.; Bickley, D. G.; McGlinchey, M. J. *Inorg. Chim. Acta* **1981**, *48*, 53.

(41) Lauher, J. W.; Hoffmann, R. *J. Am. Chem. Soc.* **1976**, *98*, 1729.

(42) (a) Sikora, D. J.; Rausch, M. D.; Rogers, R. D.; Atwood, J. L. *J. Am. Chem. Soc.* **1981**, *103*, 1265. (b) Prout, K.; Cameron, T. S.; Forder, R. A.; Critchley, S. R.; Denton, B.; Rees, G. V. *Acta Crystallogr., Sect. B* **1974**, *30*, 2290.

(43) $(CO)_5Cr[Sn[CH(SiMe_3)_2]_2]$: Cotton, J. D.; Davison, P. J.; Goldberg, D. E.; Lappert, M. L.; Thomas, K. M. *J. Chem. Soc., Chem. Commun.* **1974**, 893.

(44) $(C_2H_4)_2Ni[Sn[CH(SiMe_3)_2]_2]$: Pluta, C.; Pörschke, K. R.; Mynott, R.; Betz, P.; Krüger, C. *Chem. Ber.* **1991**, *124*, 1321.

(45) Ellis, J. E.; Chi, K.-M.; DiMaio, A. J.; Frerichs, S. R.; Stenzel, J. R.; Rheingold, A. L.; Haggerty, B. S. *Angew. Chem., Int. Ed. Engl.* **1991**, *30*, 194.

(46) (a) Calculated by subtracting the radius for phosphorus[47] from the known Zr–P distance of 2.678 Å in $[(Me_3Si)_2C_5H_3]_2Zr(Me_2PCH_2CH_2PMe_2)$.[46b] (b) Antinolo, A.; Bristow, G. S.; Campbell, G. K.; Duff, A. W.; Hitchcock, P. B.; Kamarudin, R. A.; Lappert, M. F.; Norton, R. J.; Sarjudeen, N.; Winterborn, D. J. W.; Atwood, J. L.; Hunter, W. E.; Zhang, H. *Polyhedron* **1989**, *8*, 1601.

(47) Pauling, L. *The Nature of the Chemical Bond*, 3rd ed.; Cornell University Press: Ithaca, NY, 1960.

(48) Donaldson, J. D.; Fuller, M. J. *J. Inorg. Nucl. Chem.* **1968**, *30*, 1083.

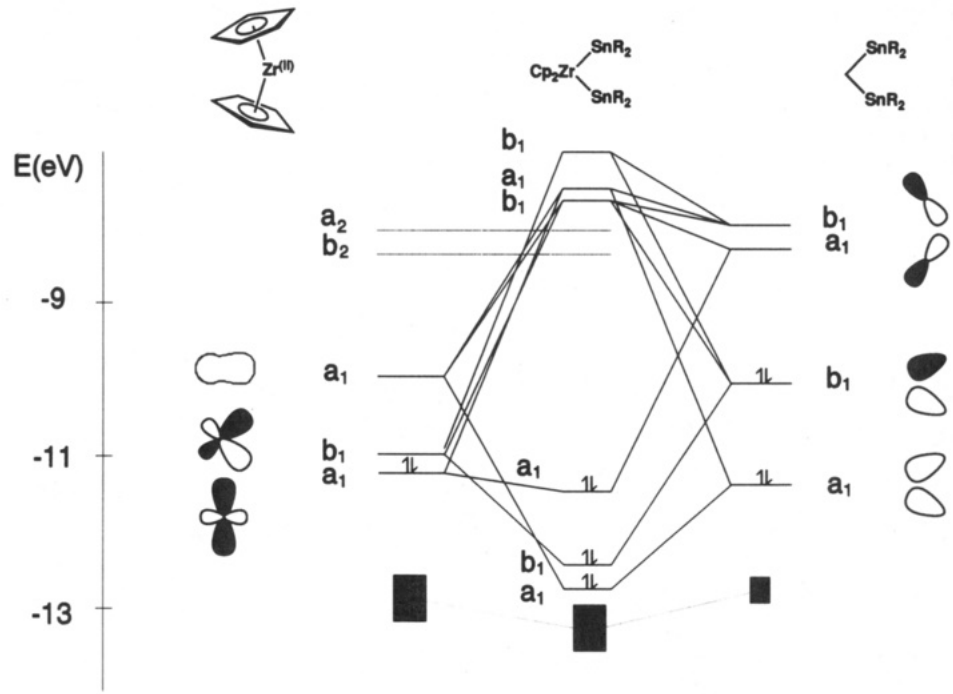


**Figure 3.** Correlation diagram for $Cp_2Zr(SnR_2)_2$.

quantitative evidence was therefore sought in the form of an EHMO calculation.

**Extended Hückel Molecular Orbital Calculations.** Much of the chemistry and bonding observed for bent metallocenes has been interpreted in terms of the well-established character of the $Cp_2M$ fragment's frontier orbitals.[41,49] Thus, a qualitative consideration of the bonding in a $d^2$ bent metallocene bonded to two $\pi$-acceptor ligands predicts a HOMO which is $\pi$ bonding in character and consists largely of the (filled) $1a_1$ orbital from the $Cp_2M$ fragment and the empty $\pi$-symmetric acceptor orbitals on the ligand (see I). An extended Hückel calculation on an idealized $C_{2v}$ representation of **1a**, $Cp_2Zr(SnMe_2)_2$, using geometrical parameters established in the structural studies on **1b**, produced a correlation diagram (Figure 3) which can be readily interpreted on the basis of the simpler qualitative approach mentioned above. On the left-hand side of Figure 3 are the fragment orbitals for $Cp_2Zr$, while on the right are the pertinent ligand group orbitals for the two stannylene donors. The $\sigma$-bonding orbitals form as expected, the symmetric and antisymmetric combinations of the tin $sp^2$ orbitals overlapping with the empty $Cp_2Zr$ $2a_1$ and $b_2$ orbitals, respectively. The calculated HOMO–LUMO gap of ~2.6 eV agrees well with the observed $\lambda_{max}$ value of 610 nm, and consistent with a formally Zr(II) center, the HOMO is relatively high in energy compared to the SHOMO, suggesting the complex might readily be oxidized. Indeed, we have observed irreversible two-electron oxidation of **1a**, both electrochemically and chemically,[50] to thus far unidentified products.

Most significant is the overlap calculated between the filled $1a_1$ orbital on $Cp_2Zr$ and the symmetric combination of the unhybridized tin $p_z$ orbitals, forming a HOMO which has a 16% Sn(p) contribution (Figure 4). This result clearly points to a bond order of between 1 and 1.5 for the zirconium–tin bonds of **1a** and **1b**, since the presence of two stannylene donors in these compounds delocalizes the Zr–Sn $\pi$ bond over the three metal atoms.

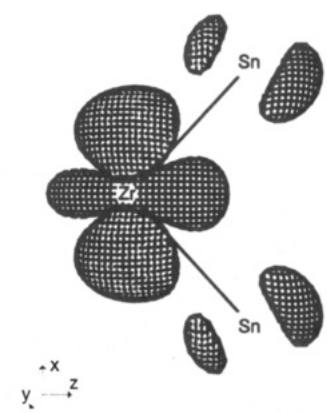


**Figure 4.** CACAO drawing of the HOMO for $Cp_2Zr(SnR_2)_2$.

**Conclusions.** This paper describes the synthesis and characterization of some stannylene adducts of zirconocene. These complexes were arrived at in an attempt to synthesize what may be thought of as a group 4/14 olefin analog, "$Cp_2Zr{=}SnR_2$". Heavy-element analogs of olefins exist within the main group of elements, but the analogy has not been extended to include group 4 based partners. While the fragment "$Cp_2Zr$" is carbene-like and may be expected to participate in $\pi$ bonding to another carbenoid moiety, evidently the presence of an extra low-energy orbital allows it to couple with a second stannylene donor to form the observed bis(stannylene) adducts, despite the great steric bulk of the stabilizing alkyl groups on tin. However, the size of these groups *is* enough to prevent complete coupling of the two stannylenes to form a tin–tin bond. Preliminary EHMO calculations indicate that the total energy of $Cp_2Zr(SnMe_2)_2$ decreases as the stannylene ligands are made to approach each other, suggesting that the formation of the bis(stannylene) adducts **1a** and **1b** might be viewed as an arrested cyclostannylation of the heavy-element olefin analogs "$Cp'_2Zr{=}SnR_2$", in analogy to the cyclopropanation of olefins. We are currently attempting to sterically stabilize a $Cp_2Zr{=}SnR_2$ species via a number of approaches, as well as synthesize other members of the bis(stannylene)zirconocene family to examine

(49) Albright, T. A.; Burdett, J. K.; Whangbo, M. H. *Orbital Interactions in Chemistry*; Wiley: New York, 1985; p 394 ff.
(50) Whittal, R. M.; Piers, W. E. Unpublished results.

further the interesting parallels between group 4 and group 14 organometallic chemistry.

**Acknowledgment.** W.E.P. thanks the Natural Sciences and Engineering Research Council of Canada for financial support of this work and Professor John D. Goddard for helpful discussions.

**Supplementary Material Available:** Tables containing full bond distance and angle data, anisotropic thermal parameters, hydrogen positional and thermal parameters, torsion angles, and mean plane data for **1b** (8 pages). Ordering information is given on any current masthead page.

OM920461W

# Differential Reactivity of the Dihydrides $Mn_2(\mu\text{-}H)_2(CO)_6(\mu\text{-}L\text{-}L)$ (L-L = $(EtO)_2POP(OEt)_2$, $Ph_2PCH_2PPh_2$) toward $Fe_2(CO)_9$ or $M(CO)_6$ (M = Cr, Mo, W). X-ray Crystal Structure of $Mn_2Fe(\mu\text{-}H)(\mu\text{-}PhPCH_2PPh_2)(CO)_{10}$

Remedios Carreño, Víctor Riera,* and Miguel A. Ruiz

*Departamento de Química Organometálica, Universidad de Oviedo, 33071 Oviedo, Spain*

Claudette Bois and Yves Jeannin

*Laboratoire de Chimie des Metaux de Transition, UA-CNRS 419, Université P. et M. Curie, 75252 Paris Cedex 05, France*

*Received May 11, 1992*

Reaction of $Mn_2(\mu\text{-}H)_2(\mu\text{-}tedip)(CO)_6$ (tedip = $(EtO)_2POP(OEt)_2$) with $Fe_2(CO)_9$ at room temperature leads to $Mn_2Fe(\mu\text{-}H)_2(\mu\text{-}tedip)(CO)_{10}$, resulting from the insertion of a $Fe(CO)_4$ fragment into an $Mn_2(\mu\text{-}H)$ bond in the parent hydride. Two isomers of this cluster are present in solution. Both have the tedip ligand bridging Mn and Fe atoms and differ in the position of the hydrido ligands, as revealed by NMR data. Reaction of $Mn_2(\mu\text{-}H)_2(\mu\text{-}dppm)(CO)_6$ (dppm = $Ph_2PCH_2PPh_2$) with $Fe_2(CO)_9$ at room temperature occurs with benzene elimination to yield $Mn_2Fe(\mu\text{-}H)(\mu\text{-}PhPCH_2PPh_2)(CO)_{10}$, the structure of which has been determined by X-ray diffraction. The cluster crystallizes in the space group $P2_1/n$ ($a$ = 9.887 (2) Å, $b$ = 35.554 (4) Å, $c$ = 9.682 (1) Å, $\beta$ = 116.93 (2)°, $V$ = 3034 (1) Å$^3$, $Z$ = 4). The structure was refined to $R$ = 0.0376 ($R_w$ = 0.0370) for 4079 reflections with $I \geq 3\sigma(I)$. The cluster contains an $Mn_2Fe$ triangle (Mn(1)–Fe = 2.9065 (5) Å, Mn(2)–Fe = 2.7247 (5) Å, Mn–Mn = 2.8917 (6) Å) triply bridged by the phosphido–phosphine ligand $PhPCH_2PPh_2$ and a hydrido ligand. Both the hydride and the phosphido group are over the Mn(2)–Fe edge. Each metal atom has three essentially linear carbonyl ligands. Mn(1) bears one carbonyl more, which has a semibridging interaction with Mn(2) (Mn(1)–C(7)–O(7) = 160.0 (3)°, Mn(1)–C(7) = 1.872 (3) Å, Mn(2)–C(7) = 2.521 (3) Å). Low-temperature UV irradiation of $Mn_2(\mu\text{-}H)_2(\mu\text{-}tedip)(CO)_6$ in the presence of $W(CO)_6$ leads to the thermally unstable cluster $Mn_2W(\mu_2\text{-}H)(\mu_3\text{-}H)(\mu\text{-}tedip)(CO)_{11}$, which can be isolated in high yield. The analogous molybdenum compound could not be isolated, but its formation could be detected by low-temperature NMR spectroscopy, which revealed the presence of two new species in solution. The formation and structures of the new clusters reported are discussed in light of the isolobal analogies.

## Introduction

Wade rules[1] and the isolobal principle developed by Hoffman,[2] Mingos,[3] and others represent a powerful tool not only for a unified understanding of the electronic and physical structures of the organic, inorganic, or organometallic molecules but also for designing rational synthetic routes to specific compounds through the building-block approach. The latter has been particularly successful in the field of di- and polynuclear transition-metal carbonyls, of which the inspired work of Stone[4] is a relevant example.

We have already considered the isolobal relationship $H^+ \leftrightarrow AuPPh_3^+$ in our general study on the reactivity of the unsaturated dimanganese hydrides $Mn_2(\mu\text{-}H)_2(\mu\text{-}L\text{-}L)(CO)_6$ (**1**, L-L = $(EtO)_2POP(OEt)_2$, (tedip);[5] **2**, L-L = $Ph_2PCH_2PPh_2$ (dppm)[6]). This has led us to the synthesis of heterometallic unsaturated clusters such as $Mn_2(\mu\text{-}AuPPh_3)(\mu\text{-}H)(\mu\text{-}L\text{-}L)(CO)_6$ or the cationic $Mn_2(\mu\text{-}AuPPh_3)(\mu\text{-}H)_2(\mu\text{-}dppm)(CO)_6^+$.[7] The structure of the latter points to a Lewis-base behavior of the neutral precursor **2**, in marked contrast with the Lewis-acid behavior expected for this electron-deficient species, as shown by

(1) Wade, K. *Adv. Inorg. Chem. Radiochem.* **1976**, *18*, 1.
(2) Hoffmann, R. *Angew. Chem., Int. Ed. Engl.* **1982**, *21*, 711.
(3) Evans, D. G.; Mingos, D. M. P. *J. Organomet. Chem.* **1982**, *232*, 171.
(4) (a) Stone, F. G. A. *Angew. Chem., Int. Ed. Engl.* **1984**, *23*, 89. (b) Stone, F. G. A. *Adv. Organomet. Chem.* **1990**, *31*, 53. (c) For a recent paper see for example: Brew, S. A.; Carr, N.; Mortimer, M. D.; Stone, F. G. A. *J. Chem. Soc., Dalton Trans.* **1991**, 811 and references therein.
(5) Riera, V.; Ruiz, M. A.; Tiripicchio, A.; Tiripicchio-Camellini, M. *J. Chem. Soc., Chem. Commun.* **1985**, 1505.
(6) (a) García Alonso, F. J.; García-Sanz, M.; Riera, V.; Ruiz, M. A.; Tiripicchio, A.; Tiripicchio-Camellini, M. *Angew. Chem., Int. Ed. Engl.* **1988**, *27*, 1167. (b) García Alonso, F. J.; Riera, V.; Ruiz, M. A.; Tiripicchio, A.; Tiripicchio-Camellini, M. *Organometallics* **1992**, *11*, 370.
(7) Carreño, R.; Riera, V.; Ruiz, M. A.; Bois, C.; Jeannin, Y. *Organometallics* **1992**, *11*, 2923.

0276-7333/92/2311-4022$03.00/0 